Journal of Thermal Analysis and Calorimetry (2022) 147:6941–6957
https://doi.org/10.1007/s10973-021-10996-9

Thermal and energy management prospects of γ-AlOOH hybrid nanofluids for the application of sustainable heat exchanger systems

S. Anitha[1] · Mohammad Reza Safaei[2,3] · S. Rajeswari[4] · M. Pichumani[1]

Received: 26 February 2021 / Accepted: 5 July 2021 / Published online: 27 July 2021

Abstract

This study focuses on double-tube heat exchanger (DTHE) to numerically examine their thermal performance by considering two types of hybrid nanofluids: (i) TiO_2-γ-AlOOH/water and (ii) TiO_2-γ-AlOOH/ethylene glycol. γ-AlOOH is an efficient material for heat transfer application. The heat exchanger consists of two tubes, which are called the inner and the outer tubes. The coolant and the hot oil, respectively, flow into the inner and the outer tubes. The volume proportion and volume fraction of nanoparticles are 90:10 (γ-AlOOH/TiO_2) and from 0.1 to 0.5%, respectively. The rates of mass flow, alongside the heat transfer rate and the pumping power, are evaluated. The employed model to solve the governing equations is a multiphase mixture, validated with earlier reports. The boundary conditions are reliable for industry deployment. When TiO_2-γ-AlOOH/water is employed rather than TiO_2-γ-AlOOH/EG, 50% improvement in heat transfer rate is obtained. It is noted that TiO_2-γ-AlOOH/EG possesses a higher (30%) pumping power than TiO_2-γ-AlOOH/water. However, to estimate the energy consumption in industrial scale, an additional analysis on pumping power of heat exchanger with EG-based coolants are needed in the future.

Graphic abstract

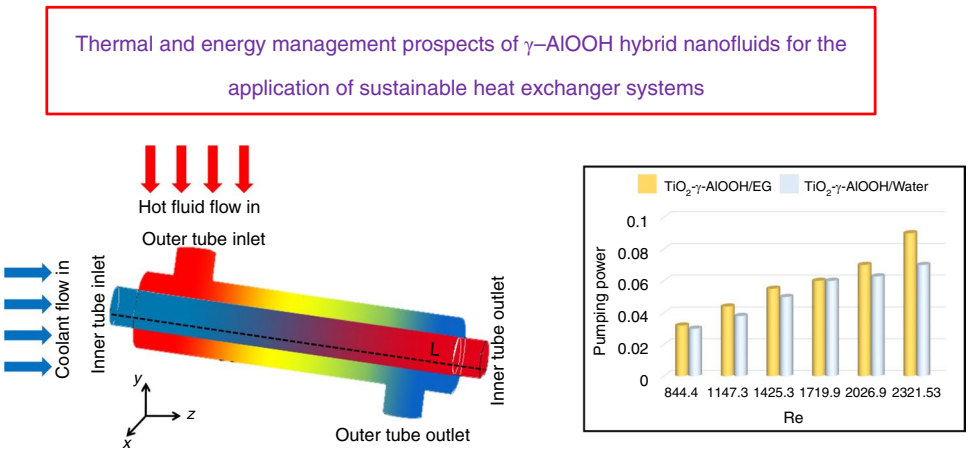

Keywords Heat exchanger · Hybrid nanofluid · γ-AlOOH · TiO_2 · Pumping power · Thermal performance

Nomenclature

A	Area of heat exchanger, m^2
C_p	Specific heat, J kg^{-1} K^{-1}
CNT	Carbon Nano Tube
D	Tube Diameter, mm
DTHE	Double-tube heat exchanger
f	Friction factor
g	Gravity force, m s^{-2}
HTP	Heat transfer performance
h	Heat transfer coefficient, W m^{-2} K^{-1}
K	Thermal conductivity, W m^{-1} K^{-1}
L	Length, mm

✉ M. Pichumani
mpichumani@srec.ac.in

Extended author information available on the last page of the article

$\dot{m}$	Mass flow rate, kg s^{-1}
n	Shape factor,-
NTU	Number of transfer units
Nu	Nusselt number, -
PP	Pumping power, W
q	Heat transfer rate, W
$\dot{Q}$	Heat convection rate
q''	Heat flux, W m^{-2}
Ra	Rayleigh number, -
Re	Reynolds Number, -
SA	Sodium Alginate
T	Temperature, ℃ (or) K
u, v, w	Velocity components, m s^{-1}
VG	Viscosity grade,-
ΔP	Pressure drop, pa
ΔT	Temperature difference, K
U	Overall heat transfer coefficient, W m^{-2} K^{-1}
$\dot{V}$	Volumetric flow rate, m^3 s^{-1}
W_{pump}	Pumping power, W
3D	Three dimensional

Subscripts

bf	Base fluid
c	Cold
c, i	Cold inlet
c, o	Cold outlet
Eff	Effective
f	Fluid
hnf	Hybrid nanofluid
h	Hot
h, i	Hot inlet
h, o	Hot outlet
m	Mixture model in Eq. (1)-(4)
max	Maximum
min	Minimum
nf	Nanofluid
s	Nanoparticle (solid particle)
w	Wall

Greek Symbols

ρ	Density, kg m^{-3}
γ	Kinematic viscosity, m^2 s^{-1}
β	Thermal expansion coefficient, K^{-1}
$\vec{v}$	Velocity vector
α	Thermal diffusivity, m^2 s^{-1}
φ	Volume fraction, %
μ	Viscosity, kg m^{-1} s^{-1}
ϵ	Effectiveness. -
η	Performance index
τ	Shear rate
$\dot{\gamma}$	Shear stress
ρ	Density

Introduction

Even though nanofluid offers higher thermal performance than base fluid, the drawbacks like lower stability, the higher pressure drop, and being cost-intensive and harmful are rectified by hybrid nanofluid (which contains more than one type of nanoparticles) (HYNF). If HYNF is used as a coolant, it will ideally contribute to improving the heat exchanger's thermal performance. Because of the broad applications of HYNF, researching HYNF is of particular interest. Different kinds of HYNFs are investigated both numerically and experimentally by various researchers. For instance, the thermal performance of non-Newtonian-based HYNF, whether with magnetic or non-magnetic nanoparticles, was studied numerically [1]. The influence of the external magnetic field on magnetite nanoparticles is stressed out. Flow and thermal performance of Cu-Al_2O_3/water HYNF were studied numerically [2]. The shrinking cylinder was used as their geometry. The skin friction coefficient was found higher for HYNF than nanofluid. With the help of the bvp4c solver, the Cu-Al_2O_3/water HYNF was studied [3]. It is stated that the increase in heat transfer rate by using the power-law velocity. Also, the friction factor of double-tube heat exchanger (DTHE) is evaluated numerically [4]

Furthermore, HTP of the heat exchanger is enhanced with the usage of copper nanoparticles [5]. Considering velocity slip and convection condition, the heat transfer performance (HTP) of HYNF over a stretching/shrinking sheet was studied [6]. The results indicated a growth in the thermal performance of HYNF when the Biot number was increased. The heat transfer rate of HYNF over a moving permeable surface was examined [7]. Radiative nanofluid with the effect of dufor and soret is studied numerically [8]. The Maxwell nanofluid and hybrid nanofluid (mixed convection flow) over a stretching sheet are analyzed [9, 10]. Temperature variations are noted in terms of source of heat, Ec (Eckert) number, Brownian motion, etc. HTP of nanofluid through porous media is numerically simulated [11]. Entropy generation of CNT/nanofluid and Casson nanofluid is investigated numerically [12, 13].

Moreover, enhancing the volume fraction of nanoparticles, the temperature profile augments. The influence of magnetic field on HYNF was reported experimentally [14]. By varying the magnetic field, the heat transfer performance was precisely observed, and at 0.05 vol. %, the higher heat transfer rate is attained.

Among many types of nanoparticles, particles like TiO_2, Al_2O_3, Cu, and Fe_3O_4 are majorly used. Observing TiO_2 nanoparticles indicates that they enhance the energy efficiency of the fluid due to their higher stability. Earlier research reports help us understand the preparation, stability, thermal conductivity, dynamic viscosity, and energy

efficiency of TiO_2 nanoparticles [15]. For instance, entropy generation of HYNF was performed in an enclosure that contained Al_2O_3-TiO_2-Cu HYNF [16]. The solutions to the governing equations were obtained by employing the finite volume method. The effect of magnetic field on nanofluid and HYNF were respectively examined [17]. It was observed that HYNF performed well as an adequate coolant when compared to nanofluid. Results of interests such as the stability and thermophysical properties of rGO-Fe_3O_4-TiO_2 HYNF were examined experimentally [18]. It was reported that HYNF, which contains TiO_2 nanoparticles, could be employed for energy and heat transfer applications with higher chemical stability. Like this, the thermophysical properties of HYNFs are widely studied [19–22]. With an increase in Re (Reynolds number), the increase in pressure drop of heat exchanger is noticed in the experimental evaluation of the HTP of zinc Ferrite/water HYNF [23], and the pressure drop reached its maximum at a higher Reynolds number. HTP of TiO_2-SiO_2 nanofluid was calculated experimentally for a tube consisting of wire coil inserts [24]. A rise was also witnessed in the thermophysical properties when the volume fraction of nanoparticles was enhanced. Moreover, the stability and dynamic viscosity of CuO-TiO_2/water HYNF were studied experimentally [25]. Besides, due to the linear reduction in its viscosity, the nanofluid experiences improved thermal performance.

Apart from the nanoparticles, the base fluid is also influential on the heat exchanger to improve its thermal performance. The following reports summarize the various base fluids used to analyze the heat exchanger's thermal performance. Ethylene glycol with multi-walled carbon nanotubes along with TiO_2 HYNF was experimentally studied [26–28]. The thermal performance of HYNF was evaluated under a range of nanoparticle volume fractions. HTP of Al_2O_3/water/polyethylene glycol mixture was investigated experimentally [29]. By considering DI water as the base fluid with a variety of nanoparticle volume fractions, the thermal efficiency of HYNF was studied experimentally [30]. The resulting pressure drop was increased upon enhancing the volume fraction of nanoparticles. Convective and rheological characteristics of HYNF with the based fluid being deionized double distilled water were explored experimentally [31]. The variations of HTP of nanofluid with the incorporation of CNT (in this case, nanofluid turns to hybrid nanofluid) are numerically examined (40). Nusselt number was increased up to 52% by using hybrid nanofluid. At 50:50 volume of water to ethylene glycol base fluid, the HTP of the heat exchanger was analyzed. The Al_2O_3 nanoparticles were dispersed in unmilled silicon carbide in their study with milled silicon carbide [32]. The milled silicon carbide with 0.8 vol. % improves the overall thermal performance by nearly 28.34%. Likewise, the heat transfer performance of nanofluid and hybrid nanofluids are studied in different types of heat exchanger systems [33–36]

Apart from these arguments, the thermal performance (to employ as a coolant) of γ-AlOOH (an aluminum oxyhydroxide) has been studied recently. For example, the synthesis method of γ-Al_2O_3 nanoparticles and γ-AlOOH nanoparticles was explored [37]. γ-AlOOH was synthesized, and it was used in electrochemical sensing applications [38]. The experimental investigations on ALOOH nanomaterial give an insight into the structure and morphology [39, 40]. The nanofluid's convective performance, which consisted of γ-AlOOH, was investigated numerically inside a wavy channel while water/ethylene glycol (EG) mixture was used as the base fluid [41]. With the increase in γ-AlOOH nanoparticles volume fraction, an improvement was witnessed in the nanofluid's thermal performance. Like water, ethylene glycol is an organic fluid with lower viscosity and volatility. Therefore it can be used as base fluid (as a coolant) [42].

To summarise the earlier reports, the following objectives are yet to be investigated.

i. How is the base fluid influential on the thermal efficiency improvement of heat exchangers having an industrial length?
ii. How do γ-AlOOH nanoparticles impact the pumping power, the overall heat transfer coefficient alongside the whole heat exchanger effectiveness?
iii. Does the choice of base fluid diminish the heat exchanger's pumping power (to extern the energy consumed by the heat exchanger)?
iv. Does the choice of base fluid become an undesired problem in the heat exchanger (energy consumption point of view)?

Besides, it is not sufficiently perceived how the choice of base fluids and nanomaterials affects the heat exchanger's energy consumption (industry length scale) regarding the second law of thermodynamics. Therefore, this study attempts to numerically investigate the HTP of the heat exchanger with double tubes by considering the following hybrid nanofluids, namely (i) TiO_2-γ-AlOOH/water (ii) TiO_2-γ-AlOOH/ethylene glycol (EG). The numerical procedure is validated with previously reported articles. The employed model to solve the governing equations is a multiphase mixture. The boundary conditions which are considered in this study are reliable to industry deployment.

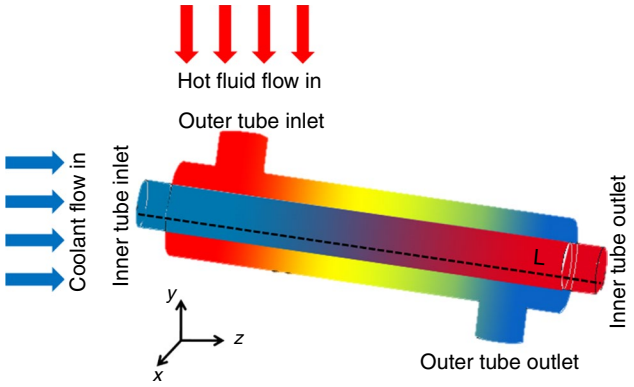

Fig. 1 The geometry of the considered problem

Definition of Double-Tube Heat Exchanger (DTHE)

The double-tube heat exchanger (DTHE) thermal performance is numerically evaluated (see Fig. 1). In DTHE, there are two distinct tubes which are called the inner and the outer. The datum of the heat exchanger is collected from the heat exchanger fabrication industry. This research aims to investigate the HTP of DTHE by employing hybrid nanofluid as a coolant rather than water (most industries use water as a coolant). The inner and outer tubes have respective lengths of 1390 mm and 1030 mm, respectively. The detailed specification of DTHE is given in our previous research article (36). The coolant passes through the inner tube with an initial temperature of 30 ℃, while the hot oil (ISO VG 68 OIL) enters the outer tube with an initial temperature of 75 ℃. Heat transfer takes place from hot oil toward the coolant. TiO_2-γ-AlOOH/water and TiO_2-γ-AlOOH/ethylene glycol HYNFs are employed as coolants to understand how the base fluid affects HTP of the heat exchanger. Since 2012, a material named boehmite (γ-AlOOH), an aluminum oxyhydroxide, has drawn many researchers' attention. It has exciting and ideal properties like good chemical stability, high surface area, and thermal stability [43].

Additionally, γ-AlOOH is a low-cost material and can be used (as a nanomaterial) as a coolant for industry deployment (heat exchanger). Based on the earlier reports, nanofluid containing TiO_2 nanoparticles can be effectively used (as coolant) for heat transfer applications due to its more extended stability [44]. Base fluids and nanoparticles are introduced in Table 1 based on their thermophysical properties. The models used to simulate the thermophysical properties of nanofluids and hybrid nanofluids are given in Supplementary Table 1. Those properties are predominantly dependent on the volume fraction of nanoparticles.

Table 1 Thermophysical properties of base fluids and nanoparticles at 293 K [41, 42]

Properties	γ-AlOOH	TiO_2	Water	Ethylene Glycol
ρ/kg m^{-3}	3050	4170	998.2	1053.3
C_p/J kg^{-1} K^{-1}	618.3	711	4182	3297.6
K/W m^{-1} K^{-1}	30	11.8	0.6	0.42
μ/kg m^{-1} s^{-1}	–	–	0.001003	0.00161

Governing equations and boundary conditions

The considered HYNFs are Newtonian and incompressible. The governing equations are determined as follows [45]:

Continuity equation

$$\frac{\partial}{\partial t}\left(\rho_m\right) + \nabla \cdot \left(\rho_m \vec{v}_m\right) = 0 \tag{1}$$

$$\vec{v}_m = \frac{\sum_{k=1}^{n} \varphi k \rho k \vec{v} k}{\rho_m}, \rho_m = \sum_{k=1}^{n} \varphi k \rho k \tag{2}$$

Here $\vec{v}_m$, ρ_m, φ_k, respectively, represent the mass-average velocity, the mixture density, and the volume concentration.

Momentum equation

To obtain the momentum equation for the mixture model, the sum of individual momentum equations representing each phase should be calculated. This can be written as:

$$\frac{\partial}{\partial t}\left(\rho_m \vec{v}_m\right) + \nabla.\left(\rho_m \vec{v}_m \vec{v}_m\right) = -\nabla p + \nabla.[\mu_m\left(\nabla \vec{v}_m + \nabla \vec{v}_m^T\right] \tag{3}$$

Here μ_m is the mixture viscosity and it is defined as

$$\mu_m = \sum_{k=1}^{n} \varphi_k \mu_k \tag{4}$$

Energy equation

$$\frac{\partial}{\partial t}\rho_m h_m + \nabla.\left(\rho_m h_m \vec{v}_m\right) = \nabla.\left(k_{eff} \nabla T\right) \tag{5}$$

Here k_{eff} stands for the effective thermal conductivity. Here $\rho_m h_m = \sum_{k=1}^{n} \varphi_k \rho_k h_k$

The equation of volume concentration corresponding to the secondary phase

The equation of volume concentration which represents the secondary phase p is determined as follows:

$$\frac{\partial}{\partial t}\left(\varphi_p \rho_p\right) + \nabla.\left(\varphi_p \rho_p \vec{v}_m\right) = -\nabla.\left(\varphi_p \rho_p \vec{v}_{dr,p}\right) \quad (6)$$

In both inner and outer tubes, it is assumed that the velocity and temperature are uniformly distributed. At the walls of the tubes, a no-slip condition is employed. Moreover, a boundary condition of the pressure outlet is employed at the tube outlets. Mathematical notation of the considered boundary conditions are as follows: For inlet: $W = 1, U = V = 0, \theta = \theta_c$. For outlet: $\frac{\partial U}{\partial X} = \frac{\partial V}{\partial Y} = \frac{\partial W}{\partial Z} = \frac{\partial \theta}{\partial Z} = 0$ and for the upper and lower wall: $U = V = W = 0, \theta = \theta_w$

The numerical procedure, validation and grid independence study

In this work, the thermal performance of DTHE is studied numerically by considering TiO_2-γ-AlOOH/water and TiO_2-γ-AlOOH/EG, respectively, as coolant. The associated partial differential equations are (governing equations) are solved by employing the finite volume method along with an upwind scheme (multiphase mixture model). The mixture model is a basic multiphase model that can be used for various applications. It can be used to model multiphase flows where the phases move at different velocities. It can be used to model homogeneous multiphase flows. Therefore, the usage of the mixture model is most relevant to the current study to investigate the heat transfer performance of fluids based on water and ethylene glycol. The convergence criteria are equal to 10^{-2} for the equations of continuity and momentum equation, while it has a value of 10^{-6} for the energy equation.

The validation of numerical procedure is required, and as such, the result of this study (Nusselt number) is compared to the earlier experimental report [46], and it is given in Fig. 2. In the earlier reported experimental study, they studied the HTP of nanofluid in a cylindrical pipe. The inner tube's length of DTHE is the same as the cylindrical pipe used in the earlier report. The uniform heat flux is considered on the inner tube's upper wall (as considered by the earlier report (35)). The range of coolant inlet temperature varies from 280 to 350 K. The coolant is chosen to be Cu/water nanofluid. The error between the earlier report and this study is 0.83% at 280 K. Therefore, it is ensured that the considered numerical procedure is valid.

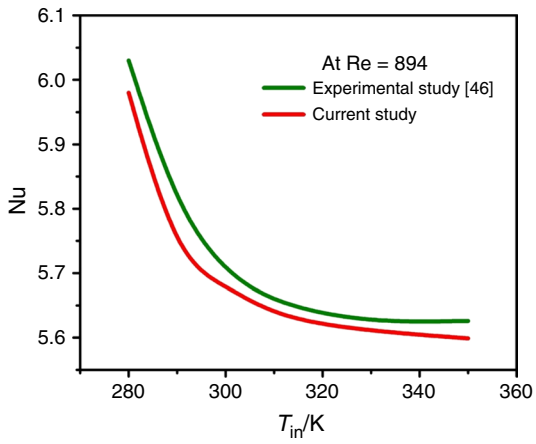

Fig. 2 The Nusselt number of this study compared to the earlier reported experimental study [35]. With constant Re = 894 and a coolant inlet temperature 280 K, error analysis between the current study and the experimental study is about 0.83%

Table 2 Grid study

Grid	30×30×105	30×30×205	30×30×305	30×30×405
T_{out}@ outer tube	48.123	47.258	46.584	46.253

The outlet temperature is measured in the outer tube to analyze the grid study (see Table 2). Since the heat exchanger's effective heat transfer performance can be optimized by emphasizing the outer tube outlet temperature. ISO VG 68 oil and coolant pass through the outer and inner tubes, respectively. The oil and coolant have respective temperatures of 75 °C and 30 °C. The outer tube temperature is tested by considering TiO_2-γ-AlOOH/water hybrid nanofluid as a coolant (with $\varphi = 0.3$, Re = 1425.3). It is seen that no considerable changes are noted after 30×30×305 grid size. Therefore, this grid size is used in the current study.

Results and discussion

DTHE is numerically investigated in terms of its thermal performance. DTHE consists of two tubes which are called the inner and the outer. The hot oil runs through the outer tube while the hybrid nanofluid/nanofluid enters the inner tube. 0.1–0.5% is the range of volume fraction of nanoparticles [45]. Since investigating the thermal performance exhibited by the heat exchanger is aimed at both regions of laminar and turbulent flow, the Re is assumed between 800 and 2400. The critical number of Reynolds number is 2000 [47].

The pressure drop experiences an increase when there is a rise in the fluid velocity. Also, the pressure drop of hybrid nanofluid ($\varphi = 0.1\%$) is lower than nanofluid ($\varphi = 0.1\%$). Besides, the pressure drop developed in water-based nanofluid and hybrid nanofluid is low compared to ethylene glycol-based. Pressure drop is identified as a critical factor that can standardize the whole heat exchanger's energy consumption. Fluid velocity, the coolant thermophysical properties alongside the system's geometry, is the crucial factor that affects the pressure drop of the heat exchanger. Figure 3 depicts the effect of fluid (coolant) velocity on the pressure drop developed in the whole heat exchanger. By varying the velocity, the Reynolds number is being calculated. It is noticed that the pressure drop is more increased at higher Reynolds numbers. Besides, ethylene glycol (EG) and the nanofluid based on it and HYNF possess higher pressure drops than water and the fluids based on it. It is due to the higher viscosity of EG. Also, it is observed that the pressure drop of the heat exchanger is seen lower with the usage of HYNF rather than nanofluid while being slightly higher than water. The same argument is reported in an earlier report [48]. It is further discussed how the heat exchanger's pressure drop is related to its pumping power. Compared to EG-based nanofluid, EG-based hybrid nanofluid possesses a lower pressure drop at Re = 2321.53. In particular, the pressure drop of the heat exchanger (at Re = 2321.53) is 667.3 for TiO_2/EG nanofluid, 667.428 for γ-AlOOH/EG nanofluid, whereas it is 416.55 for TiO_2-γ-AlOOH/EG hybrid nanofluid. Water-based hybrid nanofluid possesses a lower pressure drop than EG nanofluid in any case (at every Reynolds number). This leads to improving the heat exchanger (by varying the velocity of the fluid flow).

The friction factor experiences a decrease when there is a rise in the fluid velocity. The friction factor of hybrid nanofluid is lower compared to nanofluid. Also, ethylene glycol-based nanofluid and HYNF possess higher friction factors than water-based nanofluid.

Figure 4 illustrates how the Reynolds number affects the friction factors corresponding to base fluid, nanofluid and HYNF. The friction factor is correlated based on the difference between the inlet and outlet of the inner and outer tube. Two distinct base fluids which are water and Ethylene Glycol (EG) alongside nanofluids such as TiO_2/water, TiO_2/EG, γ-AlOOH/water, γ-AlOOH/EG and HYNFs like TiO_2-γ-AlOOH/water and TiO_2-γ-AlOOH/EG are examined. First, it is noted that coolants' friction factor decreases when there is an increment in the Re. Thermophysical property (viscosity) is a critical phenomenon that influences the friction factor of the heat exchanger and the numerical values between γ-AlOOH/water and γ-AlOOH/EG nanofluid are given in Table 3.

With this datum (from Table 3), it is understood that the viscosity of ethylene glycol (EG)-based nanofluids are 47% higher than water-based nanofluids, so does friction factor, pressure drop and pumping power. Nevertheless, as like pressure drop, the friction factor of HYNF is lower than base fluid and nanofluid.

Figures 3 and 4 show that HYNF possesses a lower pressure drop and friction factor. So, HYNF can enhance the thermal performance of DTHE rather than nanofluid and base fluid. The volume fraction of HYNF is optimized for the heat transfer rate of HYNFs, namely TiO_2-γ-AlOOH/water and TiO_2-γ-AlOOH/EG for different Reynolds numbers in respective Fig. 5a and b. With an increase in volume fraction, the heat transfer rate of both HYNFs rises. However,

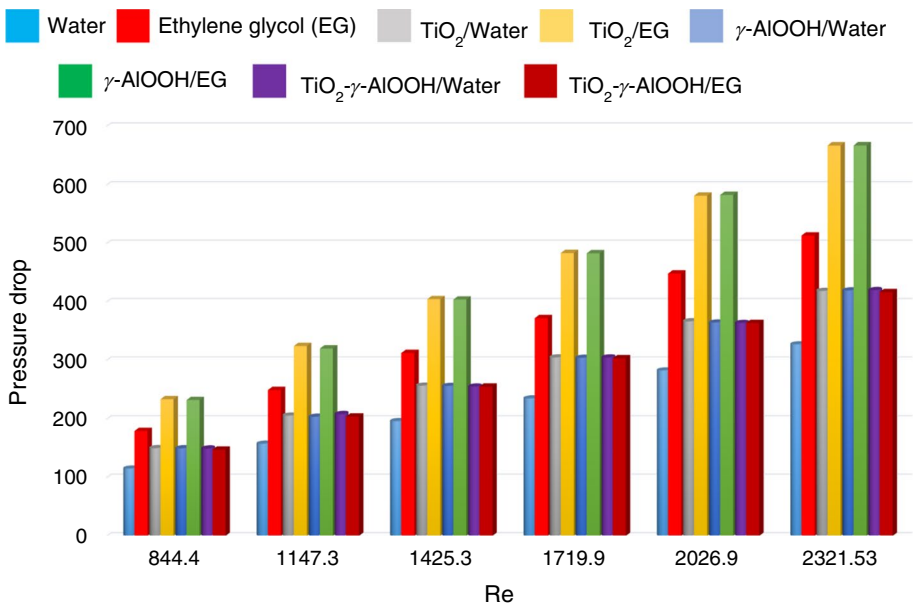

Fig. 3 Fluid velocity variations (Reynolds number) on the pressure drop in the whole heat exchanger. With an increase in Re, the pressure drop of the heat exchanger is decreased. The volume fraction of nanoparticles is fixed as 0.1 vol. %

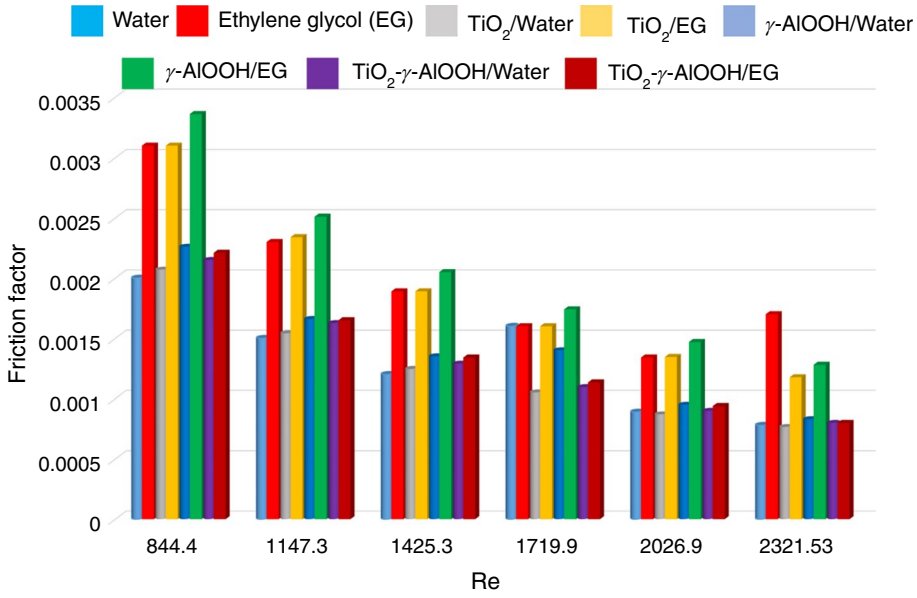

Fig. 4 The role of fluid velocity (Reynolds number) on the friction factor of the heat exchanger with volume fraction of nanoparticles is 0.1 vol. %. By increasing fluid velocity, the friction factor of the heat exchanger decreases

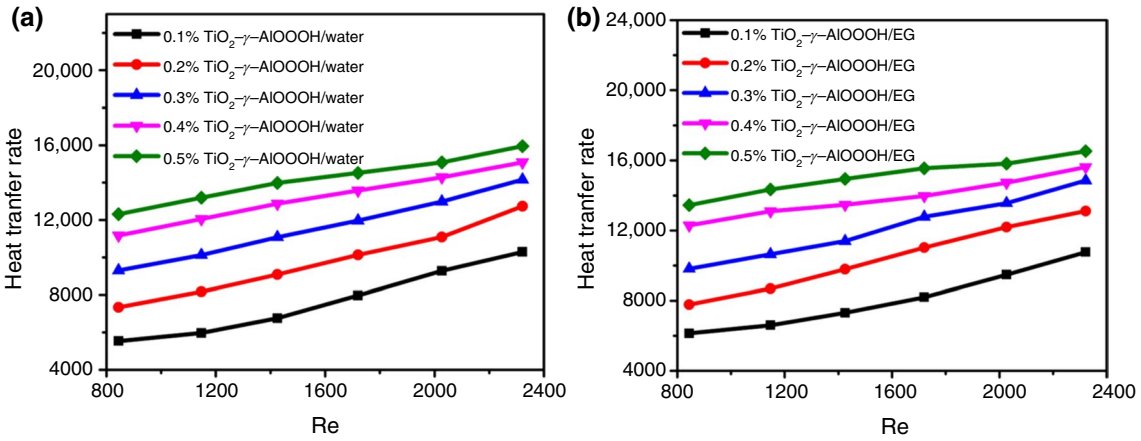

Fig. 5 The heat transfer rate of **a** TiO_2-γ-AlOOH/water **b** TiO_2-γ-AlOOH/EG based on the Re for various volume fractions of nanoparticles while having a mass flow rate of 0.2 kg s^{-1}. The volume fraction of nanoparticles varies from 0.1 vol. % to 0.5 vol. %. The rate of heat transfer of TiO_2-γ-AlOOH/EG is about ~ 10% higher than TiO_2-γ-AlOOH/water

Table 3 Viscosity of nanofluids for various volume fractions of nanoparticles

Volume fraction of nanoparticles	Nanofluids	
	γ-AlOOH/water	γ-AlOOH/EG*
0.1%	0.00125	0.00201
0.2%	0.00150	0.00241
0.3%	0.00175	0.00282
0.4%	0.00201	0.00322
0.5%	0.00226	0.00362

the increase in volume fraction augments the pressure drop and the pumping power of the DTHE. It has resulted from the addition of a higher number of nanoparticles in HYNF. Upon augmenting the volume fraction of TiO_2 nanoparticles, the stability of the HYNF rises linearly and leads to a growth in the rate of heat transfer. Also, along with an increment in the volume fraction of γ-AlOOH nanoparticles, HYNF experiences an increase in its thermophysical properties. The volume proportion of γ-AlOOH and TiO_2 nanoparticles is 90:10. The heat transfer rate is defined as follows [49]:

$$q_c = \dot{m}_c \, c_{p,c}\left(T_{c,o} - T_{c,i}\right) \tag{7}$$

$$q_h = \dot{m}_h c_{p,h}\left(T_{h,i} - T_{h,o}\right) \tag{8}$$

The mass flow rates corresponding to the coolant and the hot fluid are respectively termed as $\dot{m}_c$ and $\dot{m}_h$. Here HYNF and ISO VG 68 oil are represented as the coolant and the hot fluid, respectively. Cold outlet and cold inlet are indicated as c, o and c, i, respectively. Hot outlet and hot inlet are termed as h, o and h, i, respectively. The q between the coolant and the hot oil is in negligible difference. Therefore, $q_c = q_h = q$.

A direct proportion is indicated by Eqs. (7), (8) between the heat transfer rate of HYNF and the temperature change from the inlet to the fluid outlet. It is evident that when the volume fraction of nanoparticles is increased, the temperature difference measured between the inlet tube and the outlet tube is also intensified. Therefore, the heat transfer rate also grows linearly. However, the difference in the q between both HYNFs is not notable.

The role of Reynolds numbers on the rate of heat transfer of HYNFs for different mass flow rates ($\dot{m}$) are shown in Fig. 6a and b. The range of rate of $\dot{m}$ is from 0.2 kg s^{-1} to 1 kg s^{-1}. The heat transfer rate related to TiO_2-γ-AlOOH/water and TiO_2-γ-AlOOH/EG is illustrated in Fig. 6a and b. It is seen for all $\dot{m}$ increasing the Reynolds number causes growth in q. This figure is almost 6% for TiO_2-γ-AlOOH/water hybrid nanofluid between 844.4 and 2321.5, while the $\dot{m}$ is 0.2 kg s^{-1}. The reason is that the higher the $\dot{m}$, the larger the number of nanoparticles passing into the tube. Therefore, the heat convection between two fluids (oil and hybrid nanofluid) increases and subsequently, the q of the fluid also rises. At a lower Reynolds number (844.4), the percentage difference between TiO_2-γ-AlOOH/water and TiO_2-γ-AlOOH/EG HYNF is about 50%. Besides, as seen in Fig. 3, the pressure drop of TiO_2-γ-AlOOH/EG HYNF is higher than TiO_2-γ-AlOOH/water, and as such, the heat transfer rate of TiO_2-γ-AlOOH/EG HYNF is lower. The difference in heat transfer rate between EG-based hybrid nanofluids is about ~ 50% at the same mass flow rate and same Reynolds number.

In addition to the heat exchanger's thermal evaluation, evaluating the heat exchanger's overall performance is essential. The performance index is a critical phenomenon for studying heat transfer applications related to the heat exchanger's pressure drop. The higher pressure drop will lower the performance index (η) of the DTHE. Next, we examine the performance index of the DTHE. The heat exchanger's performance index based on the Reynolds numbers for TiO_2-γ-AlOOH/Water and TiO_2-γ-AlOOH/EG HYNF are respectively indicated in Fig. 7a, b, respectively. The performance index (η) is formulated as follows [49]:

$$\eta = \frac{q}{\Delta P} \tag{9}$$

ΔP represents the pressure drop occurring in DTHE. q denotes the heat transfer rate. The performance index (η) depends not only on q but also on the Δp that takes place in the heat exchanger (refer to Eq. 9). From Fig. 7a and b, understand that the performance index rises when both the Re and the mass flow rate augment. Furthermore, η of the DTHE is lower when TiO_2-γ-AlOOH/EG is used. Since the heat exchanger pressure drop is noted high when TiO_2-γ-AlOOH/EG HYNF is used as the coolant (see Fig. 3). Also, at a lower Re (844.4) with the $\dot{m}$ equal to 1 kg s^{-1}, the percentage difference between both HYNFs is almost 40%. The heat exchanger's performance index rises by roughly 50% when the $\dot{m}$ is increased from 0.8 kg s^{-1} to 1 kg s^{-1}.

The coefficient of overall heat transfer (U) predominantly defines the ratio between q and the temperature difference between the inlet and outlet temperature of both tubes. Figure 8 and b represent the U for various Re of TiO_2-γ-AlOOH/

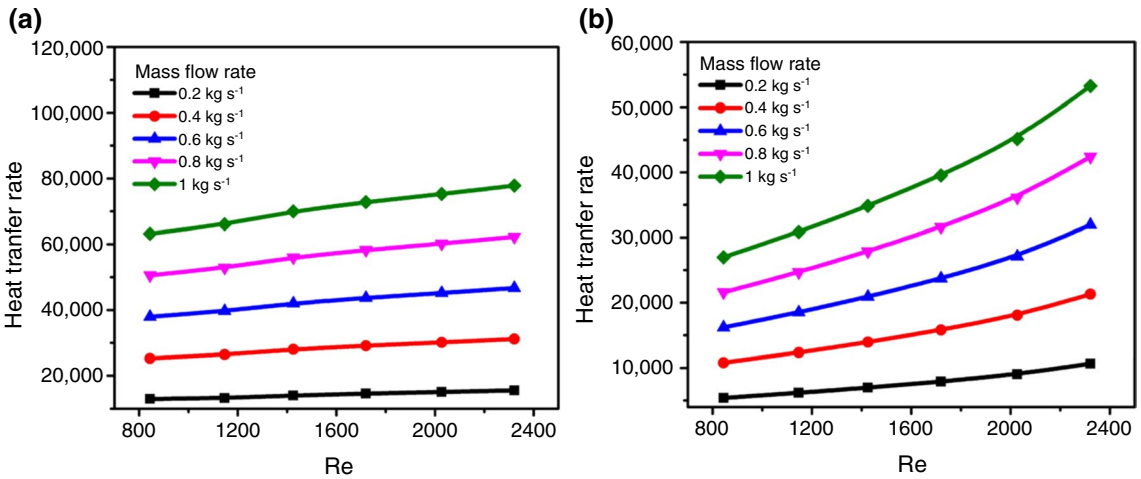

Fig. 6 The heat transfer rate based on the Reynolds number **a** TiO_2-γ-AlOOH/water **b** TiO_2-γ-AlOOH/EG at 0.1 vol. % volume fraction

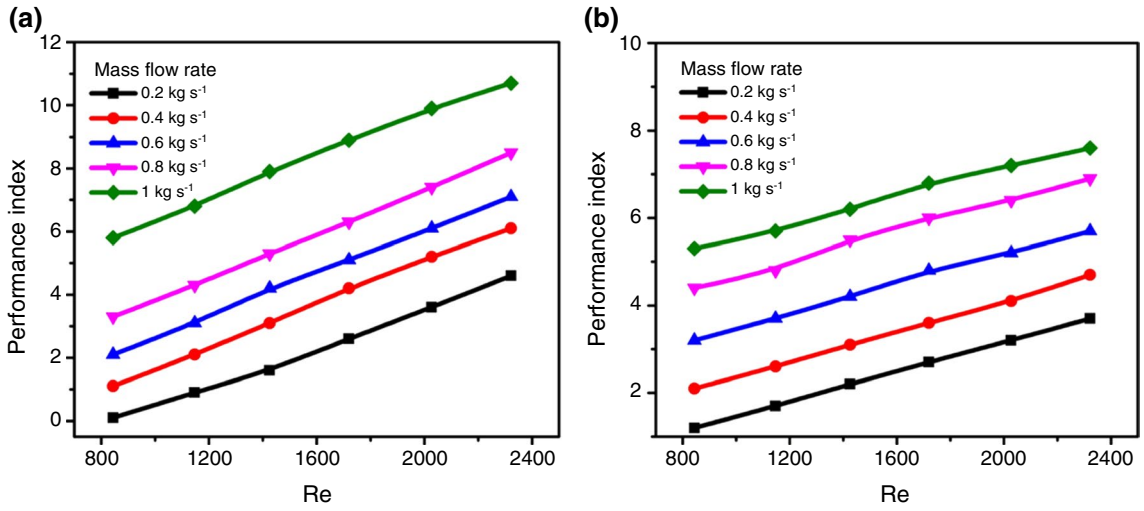

Fig. 7 The heat exchanger's performance index based on the Reynolds number **a** TiO_2-γ-AlOOH/water **b** TiO_2-γ-AlOOH/EG for different mass flow rates at 0.1 vol. % volume fraction

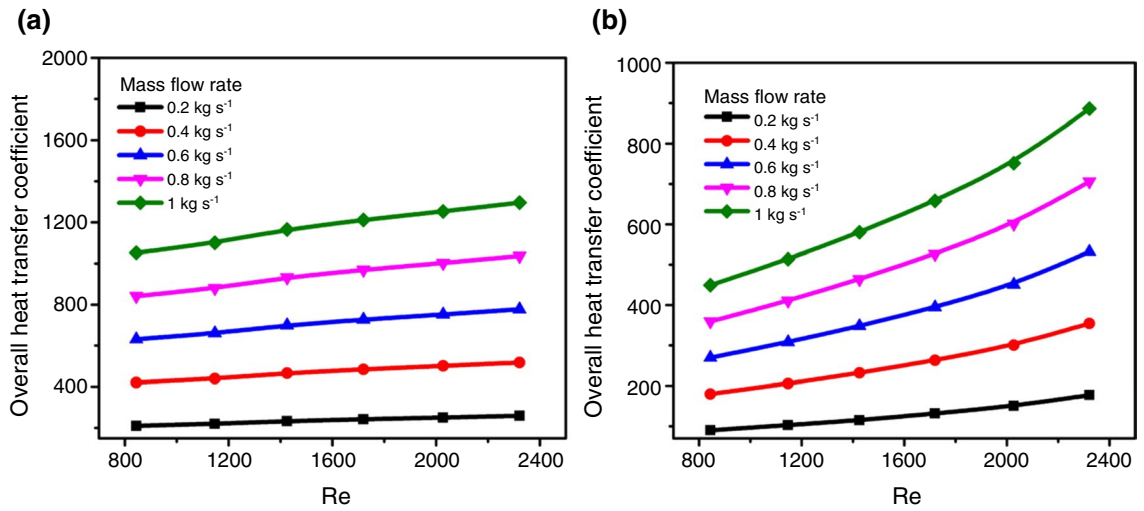

Fig. 8 The effect of Re on the coefficient of overall heat transfer of **a** TiO_2-γ-AlOOH/water and **b** TiO_2-γ-AlOOH/EG for different mass flow rates at 0.1 vol. % volume fraction

water and TiO_2-γ-AlOOH/EG HYNF, respectively. The effect of the Reynolds number on U is calculated for different $\dot{m}$. The equation below is employed to obtain U:

$$U = \frac{q}{A\Delta T_{\mathrm{LMTD}}} \tag{10}$$

here A, ΔT_{LMTD} represent the area, and the log mean temperature difference (LMTD). Where

$$\Delta T_{\mathrm{LMTD}} = \frac{\Delta T_2 - \Delta T_1}{\ln\left(\Delta T_2/\Delta T_1\right)}; \quad \Delta T_1 = T_{\mathrm{h,i}} - T_{\mathrm{c,o}}\,; \Delta T_2 = T_{\mathrm{h,o}} - T_{\mathrm{c,i}} \tag{11}$$

From Fig. 8a and b, it is easily realized that enhancing the Reynolds number alongside the $\dot{m}$. The U value is increased. What causes such an increase is the heat convection rate between the hot fluid and the coolant (HYNF), which experiences an increment when the Re and the $\dot{m}$ rise. Moreover, if the Re is even higher, the particle movement inside the tube enhances the Brownian motion, which increases the rate of heat transfer of HYNF and subsequently increases the "U". If "U" value of water-based HYNF is correlated with EG-based HYNF, water-based HYNF possesses a higher overall heat transfer coefficient. Since TiO_2-γ-AlOOH/water possesses a lower pressure drop (see Fig. 3), the heat transfer rate is higher for TiO_2-γ-AlOOH/water. An increment of

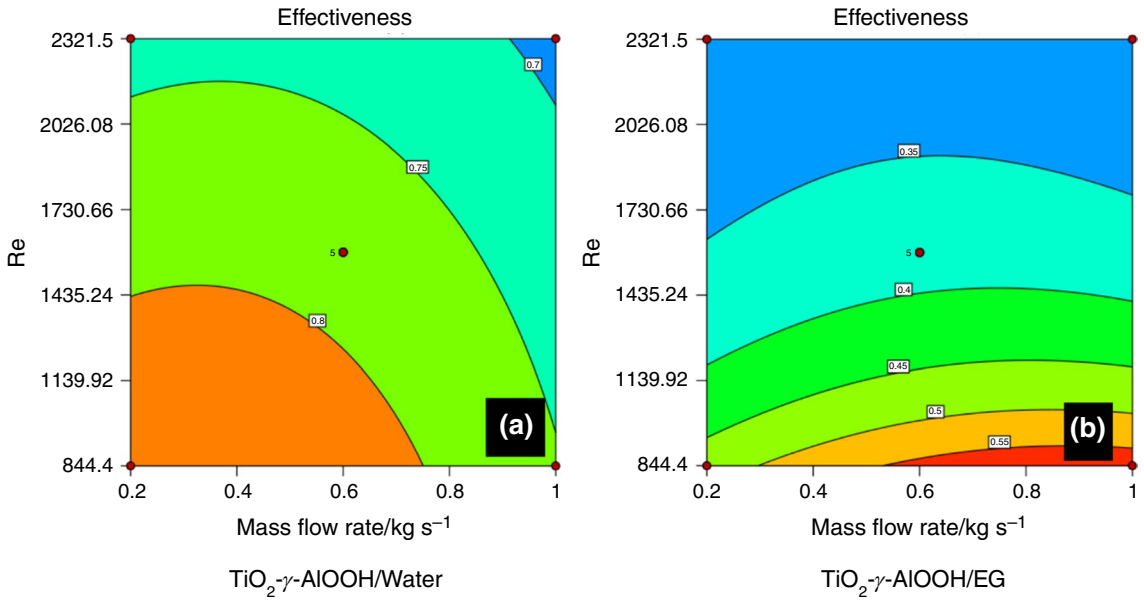

Fig. 9 The effectiveness of heat exchanger by employing **a** TiO_2-γ-AlOOH/water **b** TiO_2-γ-AlOOH/EG hybrid nanofluid as a function of Re at 0.1% volume fraction of nanoparticles

around 35% in the "*U*" is reported for TiO_2-γ-AlOOH/water HYNF at a higher $\dot{m}$ as well as a higher Re.

Figure 9 shows the heat exchanger's effectiveness contour by employing (a) TiO_2-γ-AlOOH/water (b) TiO_2-γ-AlOOH/EG HYNF in terms of Re and the rate of mass flow. Figure 10 depicts a 3D plot of effectiveness. The effectiveness of DTHE is defined as follows:

$$\varepsilon = \frac{q}{q_{\max}} \tag{12}$$

In the equation above,q and $q_{\max}$ respectively represent the heat transfer rate and its maximum value that can be derived from Eq. (13)

$$q_{\max} = C_{\min}\left(T_{\mathrm{h,i}} - T_{\mathrm{c,i}}\right) \tag{13}$$

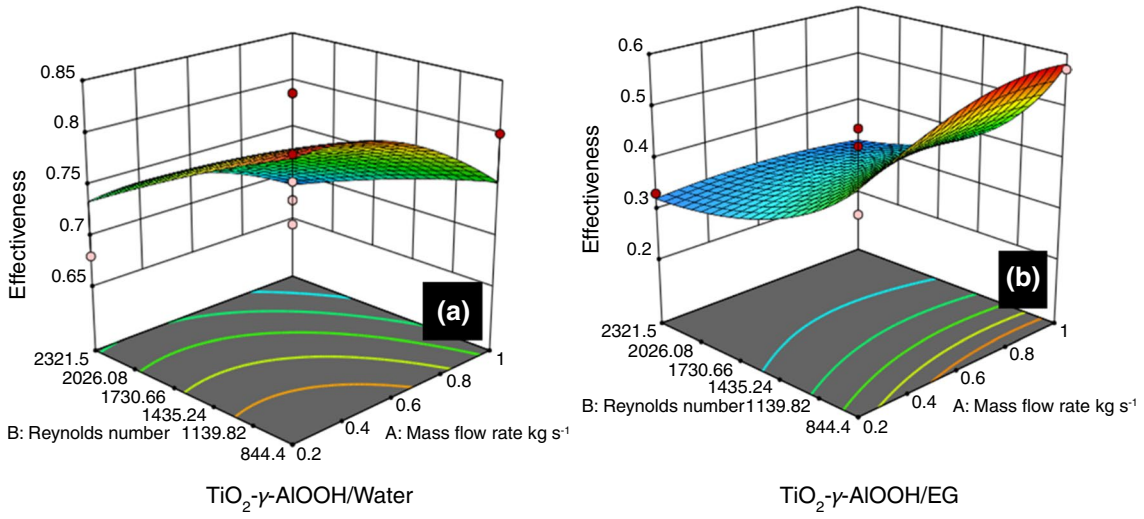

Fig. 10. 3D graph of the heat exchanger's effectiveness by employing **a** TiO_2-γ-AlOOH/water **b** TiO_2-γ-AlOOH/EG HYNF at 0.1 vol. % volume fraction of nanoparticles

The following equation determines C_{min} which is the minimum rate of heat capacity:

$$C_{min} = \min\left[C_h, C_c\right] \tag{14}$$

C_h and C_c denotes the specific heat corresponding to ISO VG 68 OIL and the coolant:

$$C_h = m_h\, c_{p,h} \tag{15}$$

$$C_c = m_c\, c_{p,c} \tag{16}$$

According to the figures, it is correct to state that as a result of enhancing the Reynolds number and mass flow rate, the effectiveness of DTHE is also increased. Also, the effectiveness of DTHE is lower when TiO_2-γ-AlOOH/EG HYNF is used. This higher effectiveness of heat exchanger is experienced higher because of the higher temperature difference monitored for the usage of water-based hybrid nanofluid. All the values are higher than 0.65 (when water is employed). Thereby the heat exchanger experience higher HTP than EG-based. Also, the percentage variation between water and EG-based coolant is 33% at a lower Reynolds number. Nevertheless, at a higher Reynolds number, it is 67%.

The blue region in Fig. 9b shows that lower effectiveness is more likely to occur than in Fig. 9a. For the same value, the 3D graph is plotted in Fig. 10.

Figures 11 and 12 show the 2D contour and 3D plot indicating the pumping power of DTHE on the Reynolds number and the mass flow rate by employing hybrid nanofluids. The pumping power of DTHE is as follows [17]:

$$\dot{W} = \dot{V}\Delta P \tag{17}$$

$\dot{V}$ represents the rate of volumetric flow, while ΔP is the pressure drop occurring in DTHE. The red shaded area in Fig. 11 denotes the higher pumping power. It is seen that for both hybrid nanofluids, the pumping power grows at higher Reynolds numbers and mass flow rates. Besides, TiO_2-γ-AlOOH/EG possesses a higher pumping power than TiO_2-γ-AlOOH/water. This since TiO_2-γ-AlOOH/EG has a higher pressure drop than TiO_2-γ-AlOOH/water. The percentage deviation in pumping power of heat exchanger is almost 25% with the usage of water-based coolant compared to EG-based coolant (at lower Reynolds number). The figure shows that the pumping power is lower with a lower mass flow rate and augments for the increase in mass flow rate.

Figure 13a shows the comparison of the outlet temperature of the outer tube between water and the hybrid nanofluid based on it for various volume fractions, and likewise, Fig. 13b shows the comparison of EG and the hybrid nanofluid based on it. DTHE exhibits a higher thermal performance when the outlet temperature (of the outer tube) is lower. The temperature is noted high when base fluid alone (water/EG) is employed as the coolant (both in fig (a) and fig (b)). Furthermore, the outlet temperature is reduced when the volume fraction of HYNF increases.

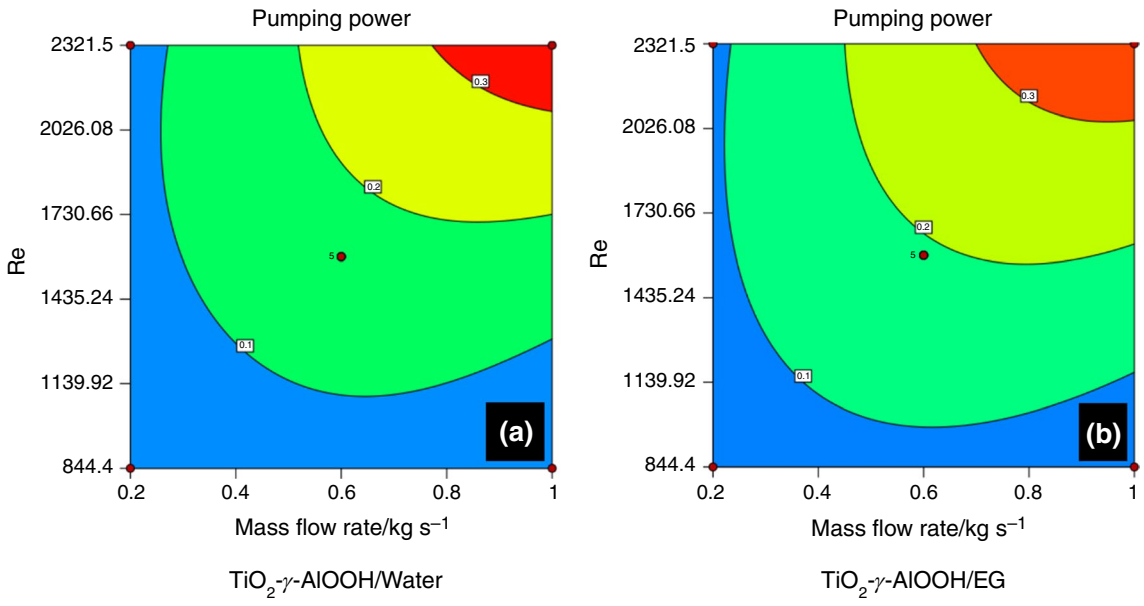

Fig. 11 The variations of the mass flow rate and the Reynolds number in pumping power of the heat exchanger by employing **a** TiO_2-γ-AlOOH/water **b** TiO_2-γ-AlOOH/EG HYNF. The volume fraction of nanoparticles is fixed as 0.1 vol. %

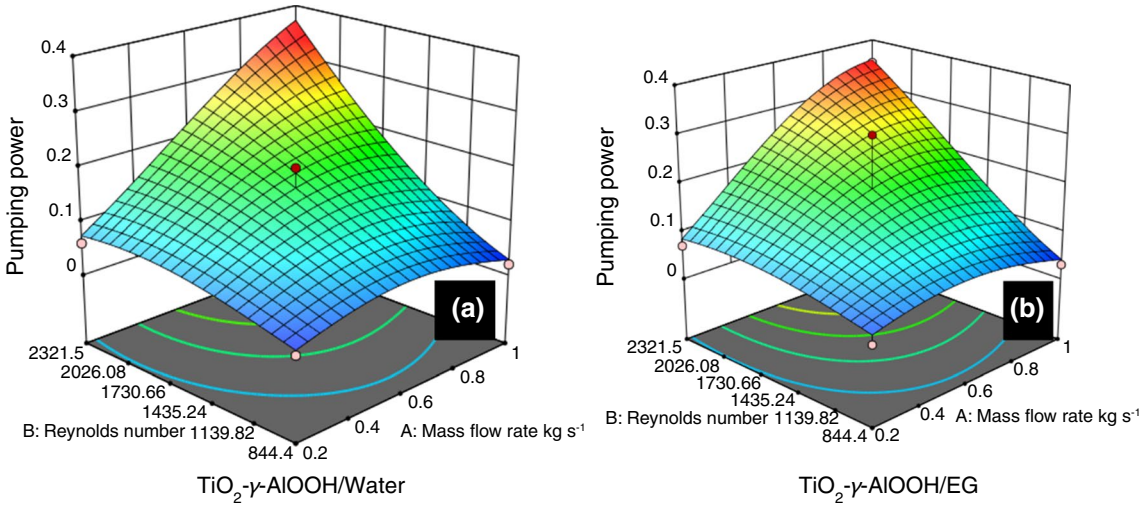

Fig. 12. 3D graph of Pumping power in terms of Re and the rate of mass flow for employing **a** TiO_2-γ-AlOOH/water (0.1 vol. %) **b** TiO_2-γ-AlOOH/EG hybrid nanofluid (0.1 vol. %)

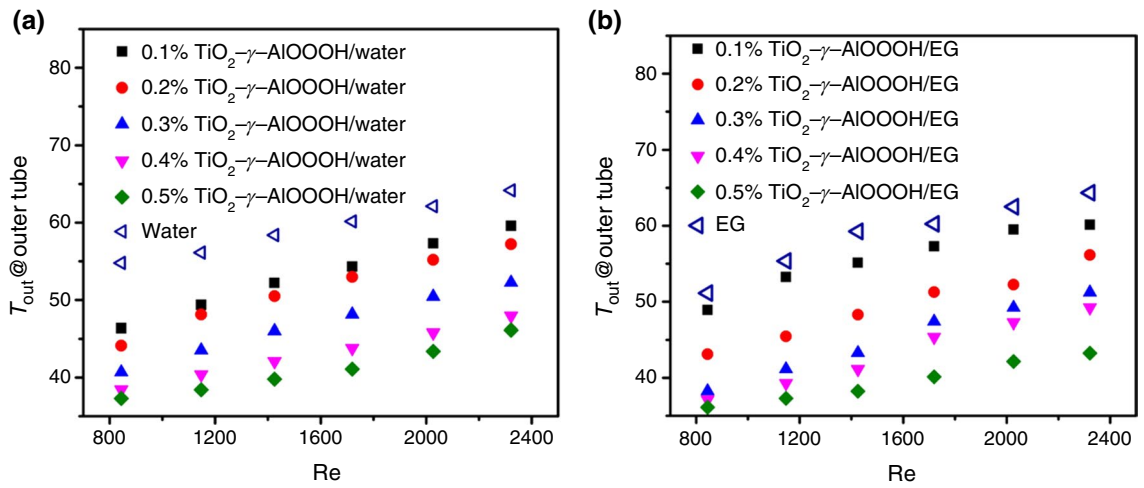

Fig. 13 The outlet temperature measured at the outer tube for different Reynolds numbers when **a** TiO_2-γ-AlOOH/water **b** TiO_2-γ-AlOOH/EG is employed as the coolant ($\varphi = 0.1\%$)

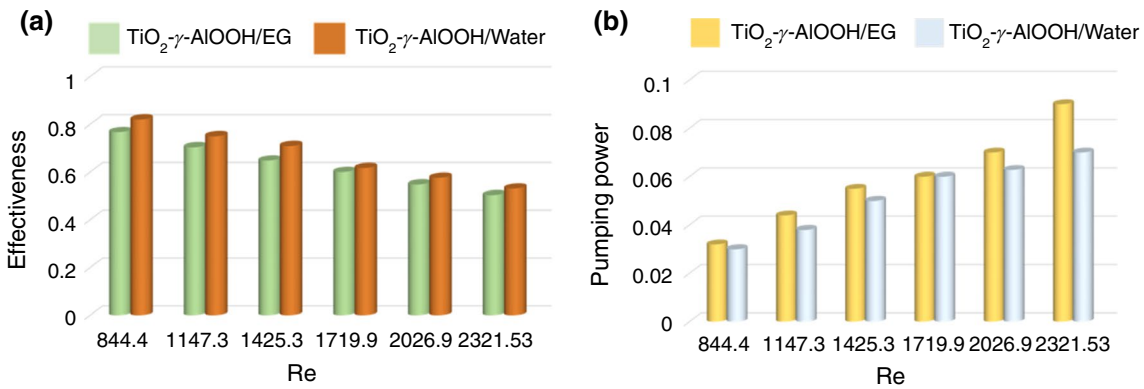

Fig. 14 **a** The effectiveness **b** the pumping power based on the Reynolds number while the mass flow rate is 0.2 kg s^{-1} and volume fraction of nanoparticles is 0.3%

Figure 14 illustrates the (a) effectiveness and the (b) pumping power of DTHE against Re. Figure 14a shows the enhancement in Reynolds number, the heat exchanger drops' effectiveness. The same trend is also reported in the earlier report [49]. It is evident from the discussions mentioned above that the effectiveness of DTHE is higher when TiO_2-γ-AlOOH/water is used as the coolant. Figure 14b shows that TiO2-γ-AlOOH/EG's pumping power is higher than TiO_2-γ-AlOOH/water HYNF. It is revealed that the pumping power experiences growth when the Re, and consequently the pressure loss, are increased. Subsequently, the pumping power is intensified at higher Reynolds numbers. An increase in the Reynolds number from 2026.9 to 2321.53 intensifies the pumping power of the hybrid nanofluid TiO_2-γ-AlOOH/EG by almost 30%. Therefore, it is concluded that water-based HYNF with a 1 kg s^{-1} mass flow rate provides higher thermal performance than EG-based HYNF.

Figure 15 shows the contours of the outer tube side temperature variations when (a) TiO_2-γ-AlOOH/water hybrid nanofluid (b) water is employed as the coolant at Re = 1425.3. ISO VG 68 oil passes through the outer tube at 75 °C. It is seen that when HYNF is used, the temperature @ outlet of the outer tube reduces to 47 ℃ and reduction is to 60 ℃ when water is used as the coolant. Therefore, it is

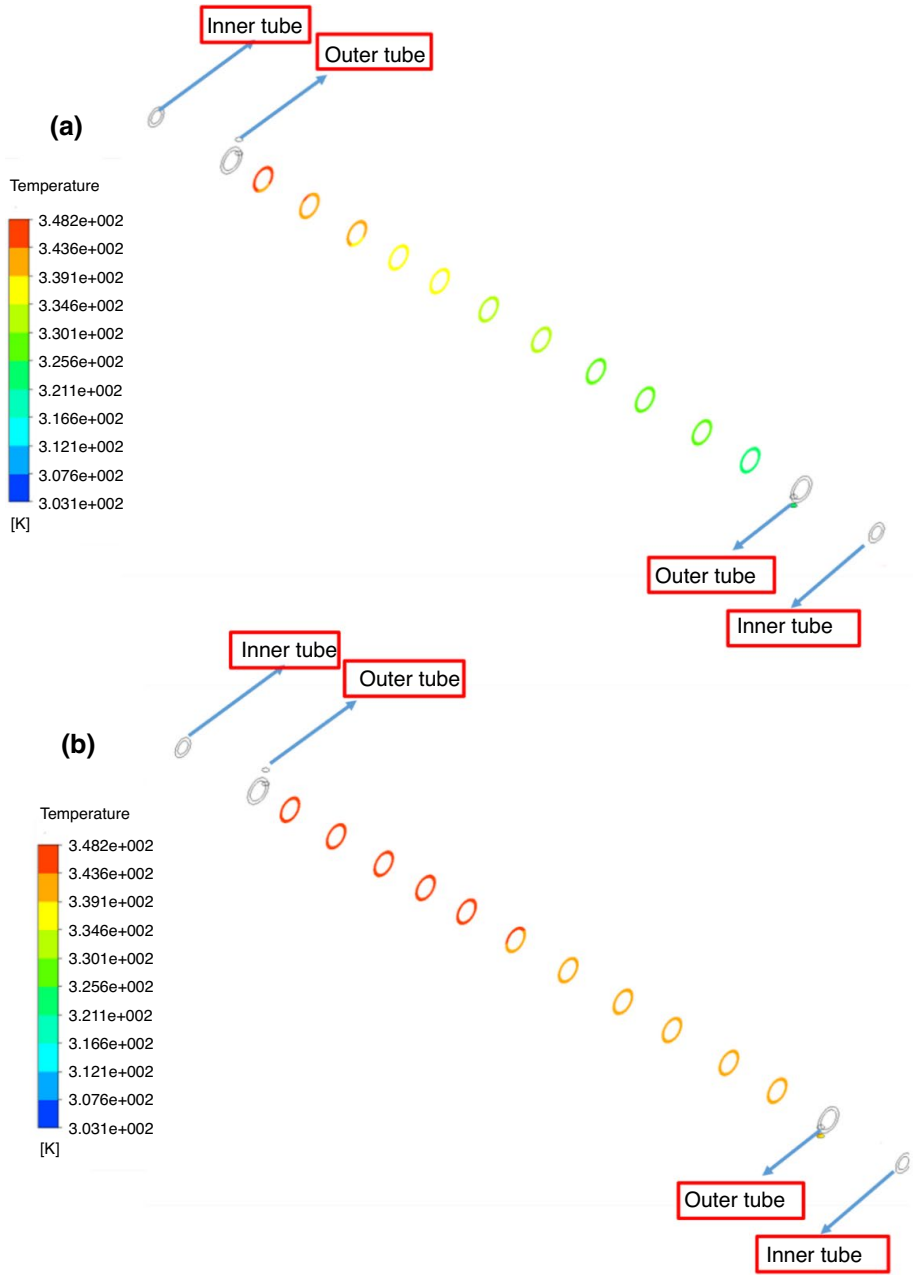

Fig. 15 The temperature contour of the outer tube when **a** TiO_2-γ-AlOOH/water HYNF with $\varphi = 0.3$ vol. % **b** water, at Re = 1425.3

shown that HYNF improves the heat exchanger in terms of its thermal performance.

The velocity vector of the outer tube is shown in Fig. 16 when TiO_2-γ-AlOOH/water HYNF is employed as a coolant with $\varphi = 0.3\%$, Re = 1425.3. At the wall, the fluid velocity reaches zero since the boundary condition is assumed to be no-slip. The velocity is more intensified in the red region. It is observed that the inlet and the outlet of the outer tube are where the hot fluid respectively enters and leaves the

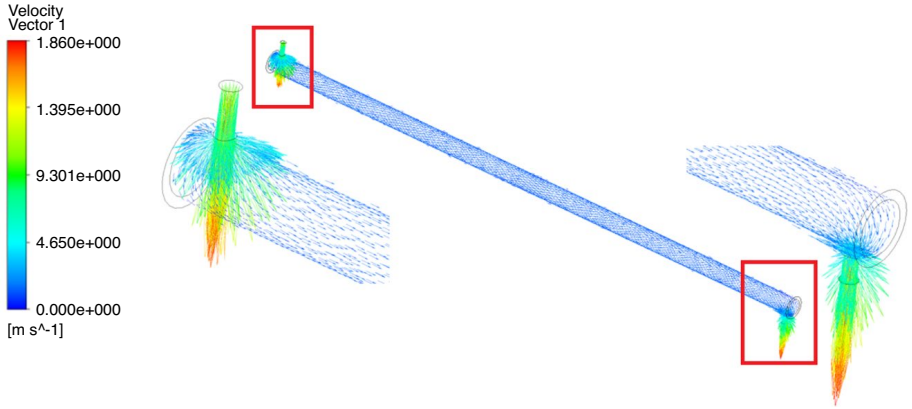

Fig. 16 The velocity vector when the coolant is TiO_2-γ-AlOOH/water HYNF with 0.3% volume fraction of nanoparticles and Re = 1425.3

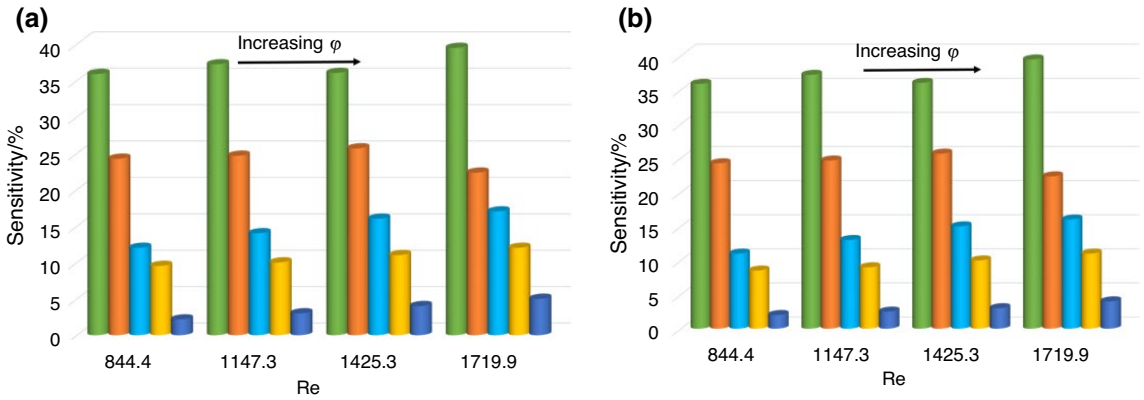

Fig. 17 The impact of various volume fractions of hybrid nanofluid on the pressure drop sensitivity. **a** TiO_2-γ-AlOOH/water hybrid nanofluid, 0.1 vol. % < φ < 0.5 vol. % **b** TiO_2-γ-AlOOH/EG hybrid nanofluid, 0.1 vol. % < φ < 0.5 vol. %

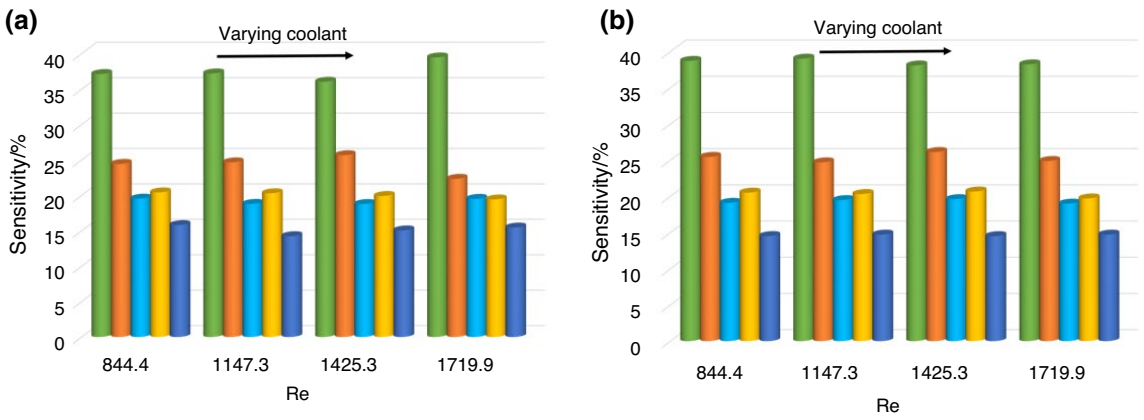

Fig. 18 The effect of various coolants (base fluid, nanofluid and HYNF) on pressure drop sensitivity. **a** Base fluid, nanofluid ($\varphi = 0.1$vol%) and hybrid nanofluid ($\varphi = 0.1$ vol%). **b** EG and EG based nanofluid ($\varphi = 0.1$vol%) and hybrid nanofluid ($\varphi = 0.1$vol%)

heat exchanger. Based on the velocity magnitude, the color changes accordingly.

Figures 17 and 18, respectively, indicate the sensitivity of pressure drop to the various volume fractions of hybrid nanofluid and coolants. The sensitivity of pressure drop can be calculated by the following Eq. [50]:

$$\text{Sensitivity} = \left(\frac{\Delta p_{\text{new}} - \Delta p_{\text{base}}}{\Delta p_{\text{base}}} \right) \times 100 \tag{18}$$

Figures 16 and 17 show that the loss in the pressure of the whole heat exchanger was most sensitive to the volume fraction of hybrid nanofluid. Therefore, from an energy consumption (of heat exchanger) point of view, the nanoparticles volume fraction should be precise in a hybrid nanofluid.

Conclusions

The thermal performance and the overall heat transfer performance exhibited by the double-tube heat exchanger associated with a hybrid nanofluid based on water or ethylene glycol are numerically investigated. γ-AlOOH and TiO_2 nanoparticles with 90:10 (respectively) volume proportion are employed [47]. Heat transfer parameters such as the mass flow rate and the Reynolds number of fluid are estimated as an attempt to understand the behavior of DTHE in terms of its rate of heat transfer, its overall heat transfer performance, and its pumping power. The pumping power is among the crucial factors of the heat exchanger that determines its thermal performance. The outcomes of this study are: γ-AlOOH is considerably influential on improving the thermal performance of HYNF in DTHE. The pumping power of DTHE rises when the Reynolds number is increased. Besides, the pumping power of TiO_2-γ-AlOOH/EG HYNF is higher than water-based HYNF. At a higher mass flow rate and Reynolds number, the overall heat transfer coefficient grows by almost 35%, where the employed coolant is TiO_2-γ-AlOOH/water hybrid nanofluid. With the increase in mass flow from 0.8 kg s^{-1} to 1 kg s^{-1}, nearly 50% is witnessed in the performance index of DTHE. As a result, TiO_2-γ-AlOOH/water HYNF is the best candidate to improve the heat exchanger's thermal and energy consumption.

Supplementary Information The online version contains supplementary material available at https://doi.org/10.1007/s10973-021-10996-9.

Acknowledgements We thank SNR Sons Charitable Trust and Sri Ramakrishna Engineering College, Coimbatore, India. This work is funded by the project scheme DST-WOS (A) (SR/WOSA/PM-86/2017). Also, this work is partly supported by the Government of India- DST INSPIRE project 04/2013/000209. We would like to thank Mr. Gopalakrishan for helping in sketching the geometry.

Author's contribution SA contributed to conceptualization, software, validation, investigation, writing-original draft. MRS contributed to writing—review and editing. SR contributed to writing—original draft. MP contributed to writing—review and editing, supervision.

References

1. Hussanan A, Qasim M, Chen ZM. Heat transfer enhancement in sodium alginate based magnetic and non-magnetic nanoparticles mixture hybrid nanofluid. Phys A Stat Mech its Appl. 2020;123957.
2. Safwa N, Arifin N, Pop I. Flow and heat transfer of hybrid nanofluid over a permeable shrinking cylinder with Joule heating : A comparative analysis. Alexandria Eng J. 2020;59(3):1787–98.
3. Safwa N, Arifin N, Pop I, Nazar R. Flow and heat transfer past a permeable power-law deformable plate with orthogonal shear in a hybrid nanofluid. Alexandria Eng J. 2020;59(3):1869–79.
4. Goodarzi M, Kherbeet AS, Afrand M, Sadeghinezhad E, Mehrali M. Investigation of heat transfer performance and friction factor of a counter- flow double-pipe heat exchanger using nitrogen-doped, graphene-based nano fluids. Int Commun Heat Mass Transf. 2016;76:16–23.
5. Waini I, Ishak A, Pop I. Transpiration effects on hybrid nanofluid flow and heat transfer over a stretching/shrinking sheet with uniform shear flow. Alexandria Eng J. 2019.
6. Safwa N, Arifin N, Pop I, Nazar R, Hafidzuddin EH, Wahi N. Flow and Heat Transfer of a hybrid nanofluid past a permeable moving surface. Chinese J Phys. 2020;66:606–19.
7. Waini I, Ishak A, Pop I. Flow and heat transfer of a hybrid nanofluid past a permeable moving surface. Chinese J Phys. 2020.
8. Jawad M, Saeed A, Kumam P, Shah Z. Analysis of boundary layer MHD Darcy-Forchheimer radiative nanofluid flow with soret and dufour effects by means of marangoni convection. Case Stud Therm Eng. 2021;23:100792.
9. Shoaib M, Asif M, Raja Z, Sabir MT. Numerical investigation for rotating flow of MHD hybrid nanofluid with thermal radiation over a stretching sheet. Sci Rep. 2020;1–15.
10. Islam S, Khan A, Kumam P, Alrabaiah H, Shah Z. Radiative mixed convection flow of maxwell nanofluid over a stretching cylinder with joule heating and heat source/sink effects. Sci Rep. 2020;1–18.
11. Shah Z, Sheikholeslami M, Kumam P. Simulation of entropy optimization and thermal behavior of nanofluid through the porous media. Int Commun Heat Mass Transf. 2020; 105039.
12. Khan A, Shah Z, Alzahrani E, Islam S. Entropy generation and thermal analysis for rotary motion of hydromagnetic Casson nanofluid past a rotating cylinder with Joule heating effect. Int Commun Heat Mass Transf. 2020;119:104979.
13. Rauof Khosravi, Saeed Rabiei, Mohammad Khaki, Mohammad Reza Safaei, Marjan Goodarzi. Entropy generation of graphene–platinum hybrid nanofluid flow through a wavy cylindrical microchannel solar receiver by using neural networks. J Therm Anal Calorim, 2021; https://doi.org/10.1007/s10973-021-10828-w.
14. Giwa SO, Sharifpur M, Meyer JP. Experimental investigation into heat transfer performance of water-based magnetic hybrid nano fluids in a rectangular cavity exposed to magnetic excitation. Int Commun Heat Mass Transf. 2020;116:104698.
15. Afridi MI, Tlili I, Goodarzi M, Osman M. Irreversibility analysis of hybrid nanofluid flow over a thin needle with effects of energy dissipation. SS symmetry. 2019;11:1–14.

16. Boulahia Z, Boulahia C, Sehaqui R. Two-phase computation of free convection and entropy generation inside an enclosure filled by a hybrid Al_2O_3 - TiO_2 - Cu water nanofluid having a corrugated heat source using the generalized Buongiorno's mathematical model : Employment of finite volume method. Mater Today Proc. 2020.
17. Emad H. Aly, I Pop. MHD flow and heat transfer neat stagnation point over a stretching/shrinking surface with partial slip and viscous dissipation: Hybrid nanofluid versus nanofluid. Powder Technol. 2020; 367:192–205.
18. Cakmak NK, Said Z, Sundar LS, Ali ZM, Tiwari AK. Preparation, characterization, stability, and thermal conductivity of rGO-Fe_3O_4-TiO_2 hybrid nanofluid: An experimental study. Powder Technol. 2020;372:235–45.
19. Giwa SO, Sharifpur M, Goodarzi M, Alsulami H, Meyer JP. Influence of base fluid, temperature, and concentration on the thermophysical properties of hybrid nanofluids of alumina – ferrofluid : experimental data, modeling through enhanced ANN, ANFIS, and curve fitting. J Therm Anal Calorim. 2020;143:4149–67.
20. Yarmand H, Gharehkhani S, Farid S, Shirazi S, Goodarzi M, Amiri A Wail Sami Sarsam, Maryan Sadet Alehashem, Mahidzal Dahari, S.N. Kazi. Study of synthesis, stability and thermo-physical properties of graphene nanoplatelet/platinum hybrid nano fluid. Int Commun Heat Mass Transf. 2016;77:15–21.
21. Bahmani MH, Akbari OA. Zarringhalam, M., Ahmadi Sheikh Shabani, G. and Goodarzi, M. Forced convection in a double tube heat exchanger using nano fl uids with constant and variable thermophysical properties. International Journal of Numerical Methods for Heat & Fluid Flow. 2019;30:3247–65.
22. Goodarzi M, Toghraie D, Reiszadeh M, Afrand M. Experimental evaluation of dynamic viscosity of ZnO–MWCNTs/engine oil hybrid nanolubricant based on changes in temperature and concentration. J Therm Anal Calorim. 2018;136:513–25.
23. Gupta M, Singh V, Said Z. Heat transfer analysis using zinc Ferrite/water (Hybrid) nano fluids in a circular tube : An experimental investigation and development of new correlations for thermophysical and heat transfer properties. Sustain Energy Technol Assessments. 2020;39:100720.
24. Hamid KA, Azmi WH, Mamat R, Sharma KV. Heat transfer performance of TiO_2–SiO_2 nanofluids in a tube with wire coil inserts. Appl Therm Eng. 2019;152:275–86.
25. Asadi A, Alari IM, Kok L. An experimental study on characterization, stability and dynamic viscosity of CuO-TiO_2/water hybrid nanofluid. J Mol Liq. 2020;307:112987.
26. Esfe MH, Rostamian SH. Rheological behavior characteristics of MWCNT-TiO/EG (40%–60%) hybrid nanofluid affected by temperature, concentration, and shear rate: An experimental and statistical study and a neural network simulating. Physica A. 2020;553: 124061
27. Yan S, Kalbasi R, Nguyen Q, Karimipour A. Rheological behavior of hybrid MWCNTs-TiO_2/EG nano fluid : A comprehensive modeling and experimental study. J Mol Liq. 2020;308:113058.
28. Peng Y, Parsian A, Khodadadi H, Akbari M. Develop optimal network topology of artificial neural network (AONN) to predict the hybrid nanofluids thermal conductivity according to the empirical data of Al_2O_3–Cu nanoparticles dispersed in ethylene glycol. Physica A. 2020;549:124015.
29. Ebaid MSY, Ghrair AM, Al-busoul M. Experimental investigation of cooling photovoltaic (PV) panels using (TiO2) nano fluid in water -polyethylene glycol mixture and (Al2O3) nanofluid in water-cetyltrimethylammonium bromide mixture. Energy Convers Manag. 2018;155:324–43.
30. Kumar V, Sarkar J. Numerical and experimental investigations on heat transfer and pressure drop characteristics of Al_2O_3-TiO_2 hybrid nano fluid in minichannel heat sink with different mixture ratio. Powder Technol. 2019;345:717–27.
31. Madhesh D, Parameshwaran R, Kalaiselvam S. Experimental investigation on convective heat transfer and rheological characteristics of Cu – TiO_2 hybrid nanofluids. Exp Therm Fluid Sci. 2014;52:104–15.
32. Ramalingam S, Dhairiyasamy R, Govindasamy M. Assessment of heat transfer characteristics and system physiognomies using hybrid nanofluids in an automotive radiator. Chem Eng Process Process Intensif. 2020;150:107886.
33. Tian Z, Abdollahi A, Shariati M, Amindoust A, Arasteh H, Karimipour A, Goodarzi M, Bach Q-V. Turbulent flows in a spiral double-pipe heat exchanger: Optimal performance conditions using an enhanced genetic algorithm. Int J Numer Meth Heat Fluid Flow. 2020;30:39–53.
34. Mohammad Hussein Bahmani, Ghanbarali Sheikhzadeh, Majid Zarringhalam, Omid Ali Akbari, Abdullah A.A.A.Alrashed, Gholamreza Ahmadi Sheikh Shabani, Marjan Goodarz Investigation of turbulent heat transfer and nanofluid flow in a double pipe heat exchanger. Adv Powder Technol. 2018; 2:273–82.
35. Dadsetani, R., Sheikhzade, G.A., Goodarzi, M. Ahmad Zeeshan, Rahmat Ellahi, Mohammad Reza Safaei. Thermal and mechanical design of tangential hybrid microchannel and high-conductivity inserts for cooling of disk-shaped electronic components. J Therm Anal Calorim. 2021;143: 2125–33.
36. Bahiraei M, Jamshidmofid M, Goodarzi M. Efficacy of a hybrid nanofluid in a new microchannel heat sink equipped with both secondary channels and ribs. J Mol Liq. 2019;273:88–98.
37. Ji G, Li M, Li G, Gao G, Zou H, Gan S, et al. Hydrothermal synthesis of hierarchical micron fl ower-like γ-AlOOH and γ-Al_2O_3 superstructures from oil shale ash. Powder Technol. 2012;215–216:54–8.
38. Yang Z, Qi C, Zheng X, Zheng J. Synthesis of Ag/γ -AlOOH nanocomposites and their application for electrochemical sensing. JEAC. 2015;754:138–42.
39. Bai L, Xu K, Jiang W, Sang M, Fang Q, Xuan S. Ensemble S of Polydopamine-Protected-Au Nanocrystals on Fe3O4 @ SiO2 @ γ-AlOOH Microflower for Improving Catalytic Performance. Applied Surface Science. Elsevier,Amsterdam, 148750 p. Available from: 2020. https://doi.org/10.1016/j.apsusc.2020.148750.
40. Beauvoir TH De, Estournès C. sintering process. 2021;194.
41. Vo DD, Alsarraf J, Moradikazerouni A, Afrand M, Salehipour H, Qi C. Numerical investigation of γ-AlOOH nano- fluid convection performance in a wavy channel considering various shapes of nano additives. Powder Technol. 2019;345:649–57.
42. Mutuku WN. Ethylene glycol (EG)-based nanofluids as a coolant for automotive radiator. Asia Pacific J Comput Eng. 2016;1–15.
43. Ali S, Ozkaymak M, Sözen A, Menlik T, Fahed A. Engineering Science and Technology, an International Journal Improving car radiator performance by using TiO_2 -water nanofluid. Eng Sci Technol an Int J. 2018;21(5):996–1005.
44. Ali HM, Sajid MU. Heat Transfer Applications of TiO_2 Nanofluids. 2017: https://doi.org/10.5772/intechopen.68602
45. Anitha S, Loganathan K, Pichumani M. Approaches for modelling of industrial energy systems : correlation of heat transfer characteristics between magnetohydrodynamics hybrid nanofluids and performance analysis of industrial length - scale heat exchanger. J Therm Anal Calorim. 2020;144:1783–98.
46. Yin Z, Bao F, Tu C, Hua Y, Tian R. Numerical and experimental studies of heat and flow characteristics in a laminar pipe flow of nanofluid. J. Exp. Nanosci. 2017;82–94.
47. Anitha S, Thomas T, Parthiban V, Pichumani M. What dominates heat transfer performance of hybrid nanofluid in single pass shell and tube heat exchanger ? Adv Powder Technol. 2019;12:3107–17.
48. Huang D, Wu Z, Sunden B. Effects of hybrid nanofluid mixture in plate heat exchangers. Exp Therm Fluid Sci. 2016;72:190–6.

49. Bahiraei M, Kiani H, Reza M. Effect of employing a new biological nano fluid containing functionalized graphene nanoplatelets on thermal and hydraulic characteristics of a spiral heat exchanger. Energy Convers Manag. 2019;180:72–82.
50. Karimi A, Afrand M. Numerical study on thermal performance of an air-cooled heat exchanger : Effects of hybrid nano fluid, pipe arrangement and cross section. Energy Convers Manag. 2018;164:615–28.

Authors and Affiliations

S. Anitha[1] · Mohammad Reza Safaei[2,3] · S. Rajeswari[4] · M. Pichumani[1]

S. Anitha
anithamaths@srec.ac.in

Mohammad Reza Safaei
cfd_safaei@yahoo.com

S. Rajeswari
rajeswarisab@gmail.com

[1] Department of Nanoscience and Technology, Sri Ramakrishna Engineering College, Coimbatore, Tamil Nadu, India

[2] Mechanical Engineering Department, Faculty of Engineering, King Abdulaziz University, Jeddah, Saudi Arabia

[3] Department of Civil and Environmental Engineering, Florida International University, Miami, FL 33174, USA

[4] Department of Mathematics, St. Joseph's College of Arts and Science for Women, Krishnagiri, Tamil Nadu, India